A numerical study of biofilm growth in a microgravity environment

A. C. Aristotelous, and N. C. Papanicolaou

Citation: AIP Conference Proceedings **1895**, 120001 (2017); doi: 10.1063/1.5007418
View online: https://doi.org/10.1063/1.5007418
View Table of Contents: http://aip.scitation.org/toc/apc/1895/1
Published by the American Institute of Physics

A Numerical Study of Biofilm Growth in a Microgravity Environment

A. C. Aristotelous[1,b)] and N. C. Papanicolaou[2,a)]

[1]*Dept. of Mathematics, West Chester University, 25 University Ave., West Chester, PA 19383, USA*
[2]*Dept. of Mathematics, University of Nicosia, 46 Makedonitissas Ave., Engomi, 1700 Nicosia, Cyprus*

[a)]Corresponding author: papanicolaou.n@unic.ac.cy
[b)]aaristotelous@wcupa.edu

Abstract. A mathematical model is proposed to investigate the effect of microgravity on biofilm growth. We examine the case of biofilm suspended in a quiescent aqueous nutrient solution contained in a rectangular tank. The bacterial colony is assumed to follow logistic growth whereas nutrient absorption is assumed to follow Monod kinetics. The problem is modeled by a coupled system of nonlinear partial differential equations in two spatial dimensions solved using the Discontinuous Galerkin Finite Element method. Nutrient and biofilm concentrations are computed in microgravity and normal gravity conditions. A preliminary quantitative relationship between the biofilm concentration and the gravity field intensity is derived.

INTRODUCTION

Understanding the effects of spaceflight on microbial communities is very important for the success of manned space missions. Bacterial communities, known as biofilms, were found in the Space Shuttle water system [1, 2] and were abundant on the Mir space station [3, 4] degrading vital working surfaces and materials [5, 6]. Their presence and management continues to be a challenge on the International Space Station (ISS) [7, 8, 9]. Their potential for increased virulence and resistance [10, 11] is a risk for crew health [12]. On the other hand, they are very important for waste water treatment which is crucial for long-term missions [13, 14].

The overwhelming majority of experimental studies to this date have taken place in simulated microgravity (SMG) or Low Shear Modeled Microgravity Environments (LSMMG) on Earth. Despite various technological advances, all of these devices are Rotating Wall Vessel bioreactors. Simply described, they consist of a cylinder which rotates on an axis parallel to the ground (perpendicular to the gravity vector) producing solid body rotation of the fluid medium. The idea is that the rotational motion is such that hydrodynamic forces counteract gravity, keeping any particles or bacterial cultures suspended in a low-shear environment [15, 16, 17]. However, despite the success and importance of SMG investigations, rotational bioreactors may not always accurately represent microgravity conditions. For example, according to [18] the gravitational force acting on particles within the RWV was measured at 10^{-2} of normal gravity (g_0) which is significantly less than that of the Earth's surface but is still orders of magnitude greater than spaceflight (10^{-4} - 10^{-6} g_0). In particular, NASA's rotating-wall perfused vessel (RWPV) and high aspect ratio vessel (HARV) were shown to be successful in providing a low-shear environment. However, some residual fluid shear stresses due to particles settling through the surrounding fluid at terminal velocity were observed. As the cell culture increases in size and density, the cumulative effect of residual stresses and pseudo-Coriolis forces, apparent in the circularly accelerated reference frame, destroy the low-shear "weightless" environment [19, 20].

In addition, experiments on the ISS with pathogenic microorganisms are costly and are a risk for astronaut health. Constraints on equipment accessibility and technical difficulties greatly limit experimentation in space [6]. Therefore, mathematical modeling is a cost effective tool that may help provide valuable insight in the physical and biological processes. There are numerous papers which use mathematical models to demonstrate how well the various rotating wall bioreactors simulate a low shear microgravity environment and or compute the positions of microcarrier beads containing the bacterial colonies in the bioreactor [11, 21, 16, 22, 23]. Other works present cell culture growth models and numerical simulations for the RWPV [24] and the HARV [25]. In [26] data from an in-flight experiment was used

Application of Mathematics in Technical and Natural Sciences
AIP Conf. Proc. 1895, 120001-1–120001-8; https://doi.org/10.1063/1.5007418
Published by AIP Publishing. 978-0-7354-1579-9/$30.00

to estimate the parameters of a logistic growth function. Klaus *et al* [27] also utilized in-flight experimental data and observed increased growth in suspended non-motile *E. coli* cultures in microgravity compared to ground controls. According to the authors, this was caused by the reduction of sedimentation and convection in the microenvironment surrounding the cells. Furthermore, they identified the ratio of cell sedimentation relative to the diffusion rate of by-products, nutrients, and the cell itself as a critical quantity without presenting a unified model.

In this work, we attempt to directly simulate the effect of weightlessness on biofilm suspensions in space using a unified approach, rather than model the SMMG conditions in experimental devices on Earth, which is mostly what we found in the literature. The phenomenological model presented here, is used to examine the case of non-motile microbial colonies suspended in a tank containing an aqueous oxygen solution. Our approach consists of a system of nonlinear partial differential equations describing the biofilm and oxygen concentrations, taking into consideration the effect of gravity. The coupled problem is solved numerically for various values of the governing parameters using the Discontinuous Galerkin Finite Element Method and results for microgravity are compared to g_0. Our results are in qualitative agreement with experimental observations found in the literature.

THE BIOFILM GROWTH MODEL

Problem Formulation

In this work we want to formulate a model to investigate how the growth of non-motile microbial colonies is influenced by the gravitational field. The microcolonies under consideration are suspended in a tank filled with water, where the nutrient (*e.g.*, oxygen) diffuses in the water-oxygen solution through the top boundary. A realistic scenario when the closed tank is not completely full, and the remaining space is occupied by air.

For our purposes we assume no flow and for simplicity a two-dimensional geometry, *i.e.*, there is no variation in the y-direction. We consider an orthogonal closed tank of width L and height H measured from the bottom left corner of the tank (see Figure 1). Oxygen enters the tank from the top boundary only and the effect of gravity is assumed to be constant. In reality, the actual body force on fluids and any other object contained in the ISS (including the station itself) contains a time-dependent component due to gravity modulation [28]. However, here we assume its effect to be negligible since large modulation amplitudes are required to cause motion in our framework [29]. Each bacterial

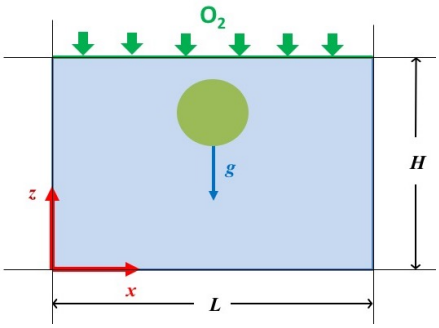

FIGURE 1: Two-dimensional representation of the tank geometry, with a suspended spherical biofilm colony. The tank has height H and width L and oxygen diffuses into the system from the top boundary

colony is modeled as a single non-deforming solid sphere suspended in the surrounding fluid (see Figure 1). The growth of the colony is dependent on the abundance of oxygen. We assume that nutrient absorption follows Monod kinetics and that the bacterial colony exhibits logistic growth. The oxygen diffusion rate is taken to be uniformly constant within the fluid and biofilm tissue – a valid assumption for small molecules. It is assumed that some biofilm diffusion occurs at the biofilm-solvent interface, albeit at orders of magnitude smaller than the oxygen diffusion rate. In addition, we make the assumption of quasi-equilibrium, since the diffusion-reaction equilibration time is of order of seconds, whereas the time scale of biological growth is of order of days [30].

The position of a colony depends on whether sedimentation occurs, a gravity-dependent phenomenon. According to Stoke's law, the terminal velocity $\boldsymbol{V_T}$ of a spherical particle of density ρ_P falling freely under gravity through fluid

of density ρ_F is

$$\boldsymbol{V_T} = \frac{2}{9}\frac{R^2\boldsymbol{g}}{\mu}(\rho_P - \rho_F) \tag{1}$$

where R is the radius of the sphere, $\boldsymbol{g}$ is the gravity vector, and μ the fluid viscosity [31]. More general formulas for non-spherical particles can be found in [32]. For sedimentation to occur, the particle, *i.e.*, the bacterial colony, must be denser than the surrounding fluid. In that case, the colony falls through the solvent with sedimentation velocity directly proportional to the intensity of the gravity field. This means that the weaker the gravitational field, the closer the colony remains to the oxygen source for a longer time period. Furthermore, the particle's velocity increases with the square of its radius. However, under the assumption of constant density, this implies that as the colony (biomass) grows, its volume and therefore its sedimentation velocity increases.

The Governing Equations

Considering all of the above we write the following system of equations describing our model

$$u_t = D_b \triangle u + \alpha\frac{\partial u}{\partial z} + r_b\left(\frac{v}{v+K}\right)u(1-u)\,, \tag{2}$$

$$0 = D_n \triangle v - ur_n\left(\frac{v}{v+K}\right), \tag{3}$$

where u and v are the biofilm and nutrient volume fractions in the domain $\Omega = [0, L] \times [0, H]$. D is the diffusion coefficient and r is the Monod coefficient with K being the nutrient half-saturation rate. The subscripts b and n denote quantities appearing in the equations for the biofilm Eq. (2) and nutrient Eq. (3) respectively.

The dimensionless coefficient of the gravity effect is given by $\alpha = mg/\nu$, where m is the mass of biofilm colony per unit surface, $g = |\boldsymbol{g}|$ is the intensity of gravity field and $\nu = \mu/\rho_F$ is the kinematic viscosity of the solvent. Changing the value of α allows us to simulate any gravity environment of our choice.

Since we have a tank with rigid walls, no flux conditions are prescribed on $\partial\Omega$ for the biofilm equation (2), whereas for the nutrient equation (3), a Dirichlet boundary condition is applied on the top boundary along with no flux conditions on the remaining sides.

NUMERICAL METHOD

Since our governing equations are nonlinear, inhomogeneous and do not possess analytical solutions, robust, accurate and efficient numerical methods are required. Consequently, we employ high-order discontinuous Galerkin (DG) finite-element (FE) numerical schemes. Since finite elements generate a variational formulation of (2) and (3), the effects of any colony supported functions, can be readily handled using high-order numerical quadratures in conjunction with compatible meshes. Mesh adaptivity can be employed, if required, to better resolve the effect of a colony on the oxygen profile [33, 34]. High-order solution approximations can be obtained by using higher degree basis functions. A comprehensive review of DG methods for the spatial discretization of elliptic PDEs can be found in the literature [35].

We now briefly describe the specific numerical method utilized to solve the governing equations in this study. For the time-stepping, the well-known θ-method is employed – the choice of $\theta = 0.5$ corresponds to the Crank-Nicholson method which provides in theory second-order accuracy in time. We arrive at the following fully discrete scheme for system (2), (3): Find $(u_h, v_h) \in V_h^r$ such that,

$$\begin{aligned}(u_h^n - u_h^{n-1}, w) = Dt \times \Big\{ &-\theta D_b \mathcal{B}_h^b(u_h^n, w) - (1-\theta) D_b \mathcal{B}_h^b(u_h^{n-1}, w) \\ &+ \theta\left(\alpha\partial_z u_h^n + r_b\left(\frac{v_h^n}{v_h^n + K}\right)u_h^n(1-u_h^n), w\right) + (1-\theta)\left(\alpha\partial_z u_h^{n-1} + r_b\left(\frac{v_h^{n-1}}{v_h^{n-1}+K}\right)u_h^{n-1}(1-u_h^{n-1}), w\right)\Big\},\end{aligned} \tag{4}$$

$$D_n \mathcal{B}_h^n(v_h^n, w) = -\left(u_h^{n-1} r_n\left(\frac{v_h^n}{v_h^n + K}\right), w\right), \tag{5}$$

where $w \in V_h^r$ is a DG basis function and V_h^r is the DG finite dimensional space [35] consisting of piecewise polynomial elements of degree, $q = r - 1$. The usual L^2-inner product is denoted by $(\cdot, \cdot)$ and $\mathcal{B}_h^b(\cdot, \cdot)$, $\mathcal{B}_h^n(\cdot, \cdot)$ is the DG bilinear

form corresponding to the Laplacian operator in variational form with prescribed BCs [36]. The qth-order DG basis polynomials, *e.g.*, $q \in \{1, 2, 3, 4\}$, provide accuracy that is $O(h^r)$ for the L^2-norm of the spatial error at each time step, with h being the mesh discretization parameter. Here, we have used quadratic polynomials which, in theory, gives us an L^2-spatial error that is $O(h^3)$. Use of the symmetric interior penalty variant of DG-FE [35] results in symmetric positive-definite mass and stiffness matrices which allow the use of efficient iterative solvers and preconditioners.

Implementation

Equations (4), (5) are solved sequentially by considering the biofilm concentration in (5) at the previous time step effectively decoupling the system. The various matrices need only be assembled once – as long as the mesh remains unchanged – at the initial time which makes the scheme efficient.

The code was written in C++ and makes use of the deal.II software library [37, 38, 39]. One of the advantages of using the deal.II framework is that the resulting code is dimension-independent. In our case the nonlinear terms were treated using a fixed-point method with relaxation. Other advantages of the library is that one can easily choose from a rich collection of linear algebraic system solvers and preconditioners. Here, a conjugate gradient solver with SSOR with relaxation preconditioning is employed.

NUMERICAL RESULTS

In Figure 2 the transient profile of a simulated biofilm colony and the corresponding nutrient concentration for $\alpha = 0.2$ are presented. As an initial biofilm distribution the colony was assumed to be a disk D of radius 0.1 centered at $(0.5, 0.8)$ with $u_0 = 0.1$ inside the disk and $u_0 = 0$ outside. We observe that the biofilm colony has a significant effect on the nutrient distribution, consuming the oxygen in its vicinity. At the same time, this limits nutrient access and availability for the cells which are further from the oxygen source.

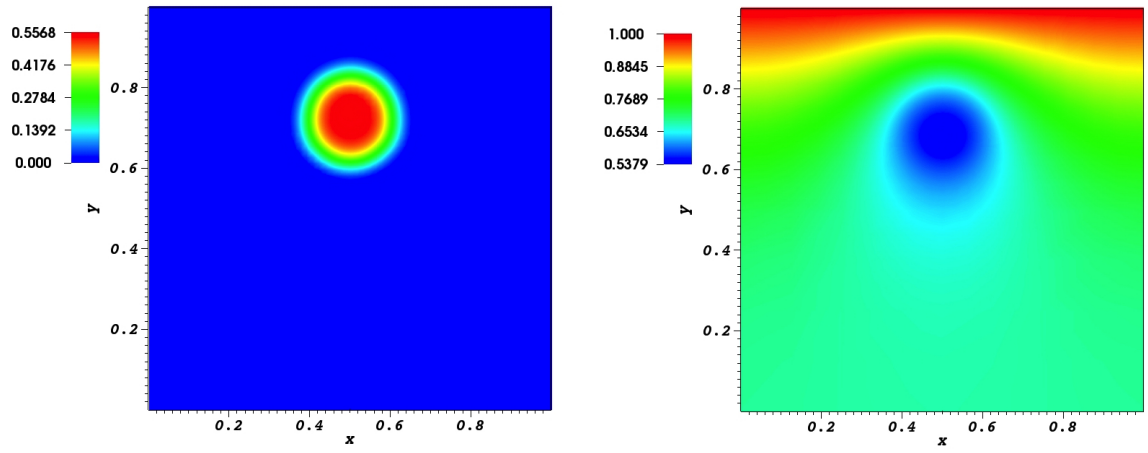

FIGURE 2: Simulation results for the case $\alpha = 0.2$, $D_n = 0.1$, $D_b = 0.001$, $K = 0.5$, $r_b = r_n = 10$. Scheme parameters: $T = 0.4$, $h = 0.015625$, $Dt = 0.000133333333$, $\theta = 0.5$, $q = 2$. Left panel: Biofilm concentration; Right panel: Nutrient profile

Evolution in Time: $g = 0$ vs $g > 0$

To illustrate how the gravitational field (or its absence) affects the growth of the bacterial colony, simulations are presented for $\alpha = 0$ ($g = 0, \mu g$-environment) and $\alpha = 0.6$ ($g > 0$) in the top rows of Figure 3 and Figure 4 respectively. For $\alpha = 0$, the bacterial colony remains at its initial location close to the nutrient source, irrespective of growth. For $\alpha = 0.6$, due to the effect of the gravitational field, the colony falls towards the bottom of the container further away from the nutrient source. We observe that the bacterial colony *grows at a* ***slower rate*** *compared to the microgravity case*. This is in agreement with the published experimental results in [27].

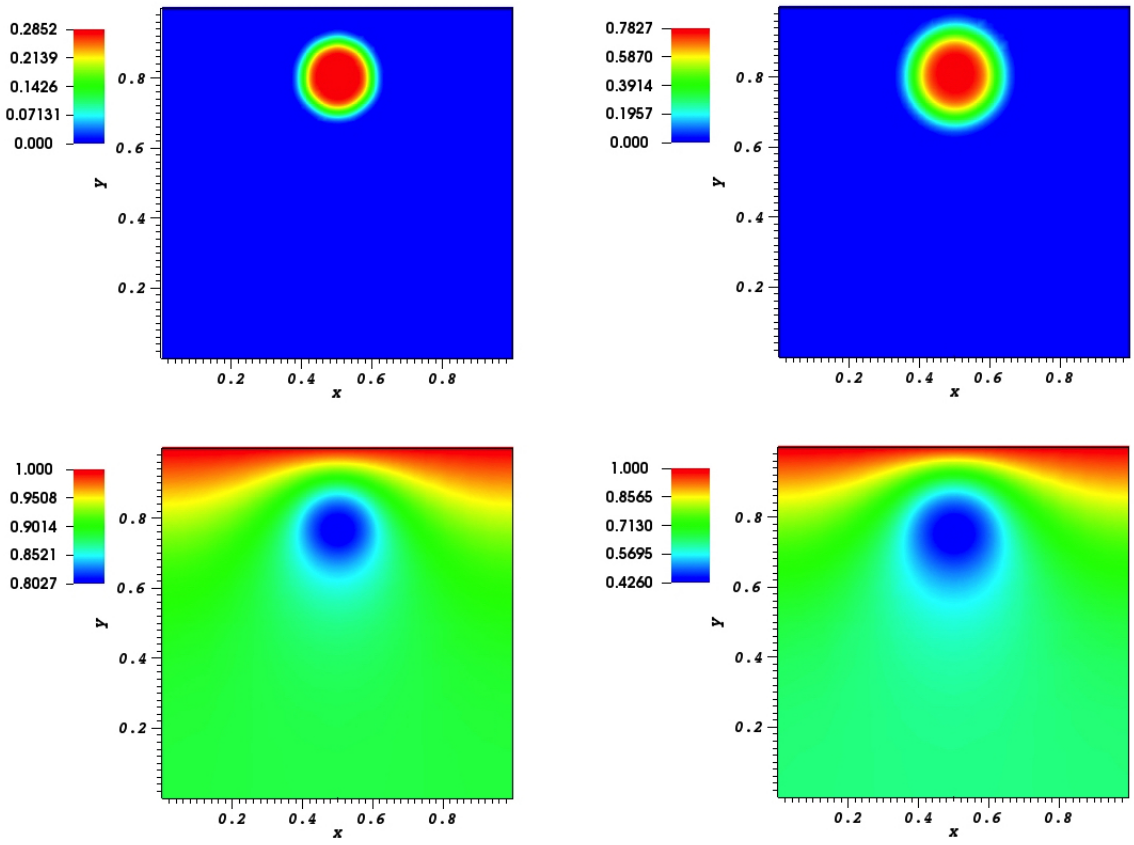

FIGURE 3: Evolution in time for $\alpha = 0$. Top row biofilm, bottom row nutrient. Left panel: $t = 0.2$, right panel: $t = 0.6$. Governing parameters: $D_n = 0.1$, $D_b = 0.001$, $K = 0.5$, $r_b = r_n = 10$. Initial condition: $u_0 = 0.1$ on $D = \{(x, y) \in \mathbb{R}^2 | (x-0.5)^2 + (y-0.8)^2 = 0.01\}$ and $u_0 = 0$ elsewhere. Scheme parameters $h = 0.015625$, $Dt = 0.0001$, $\theta = 0.5$, $q = 2$

Now, we examine how the presence or absence of gravity affects the nutrient concentration profile. Our results are presented for $\alpha = 0$ and $\alpha = 0.6$ in the bottom rows of Figure 3 and Figure 4 respectively. Once again, we observe the definitive effect of the bacterial colony. As time increases, the nutrient minimum value for $\alpha = 0.6$ decreases at a more rapid rate compared to the case $\alpha = 0$. Furthermore, for $\alpha = 0.6$ the effect of the colony on the nutrient distribution in the region between the colony and the bottom boundary is much more pronounced compared to $\alpha = 0$. Should a second colony be present between the current one and the bottom of the tank, we expect its growth to be hindered due to the effect observed in Figure 4.

In microgravity however, due to proximity of the colony to the nutrient source there is more oxygen available and it is also more evenly distributed around the colony. Thus the colonies are expected to add more mass [33].

Quantifying the Biofilm Dependence on α

The previous simulations clearly demonstrate the important effect of the gravitational field on both the biofilm and nutrient profiles. In the current subsection we present a quantitative relationship describing the dependence of the biofilm concentrations on the gravity parameter α. The total biofilm quantity (integral over the entire domain) at time $T = 0.6$ is computed for different α values. Our results are presented in Figure 5 along with the derived best fit curve. As expected, this investigation confirms the inhibiting effect of the gravitational field intensity on biofilm growth for this setting. Moreover, it indicates that the total biofilm in the tank decreases with the dimensionless parameter α.

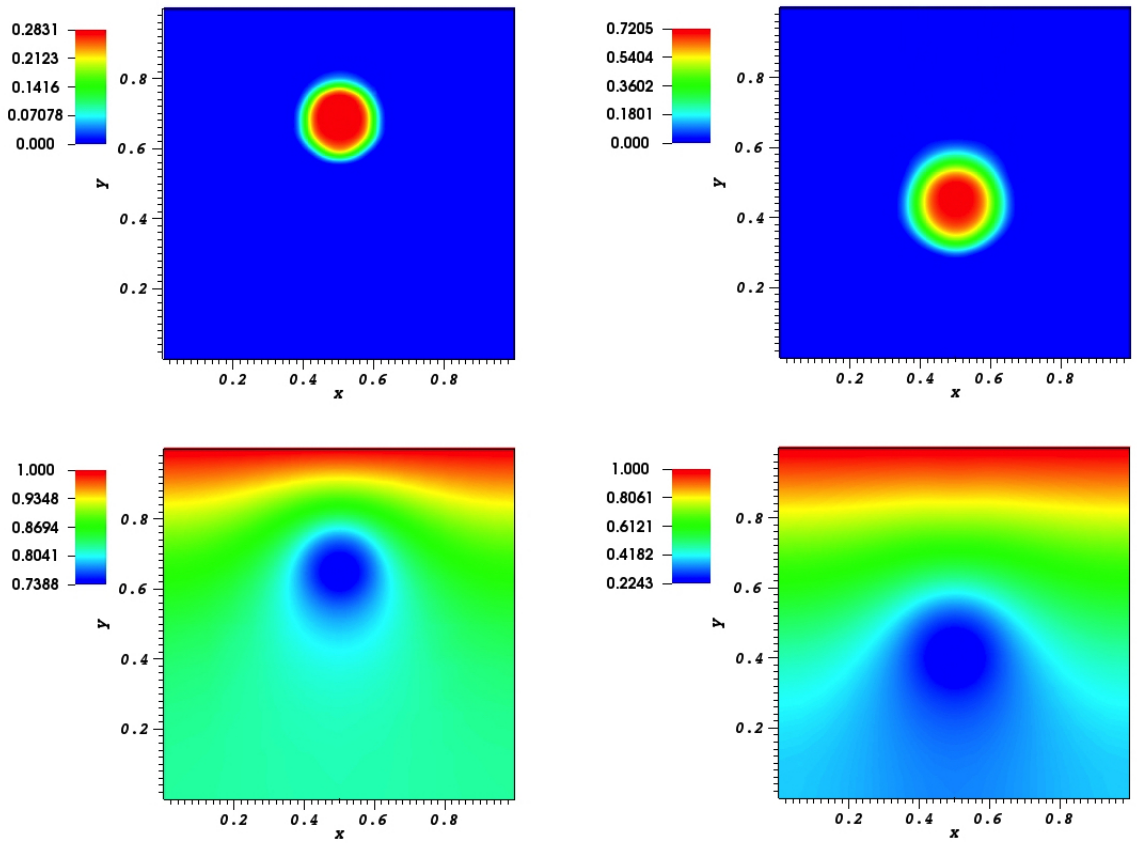

FIGURE 4: Evolution in time for $\alpha = 0.6$. Top row biofilm, bottom row nutrient. Left panel: $t = 0.2$, right panel: $t = 0.6$. Governing parameters and initial condition as in Figure 3

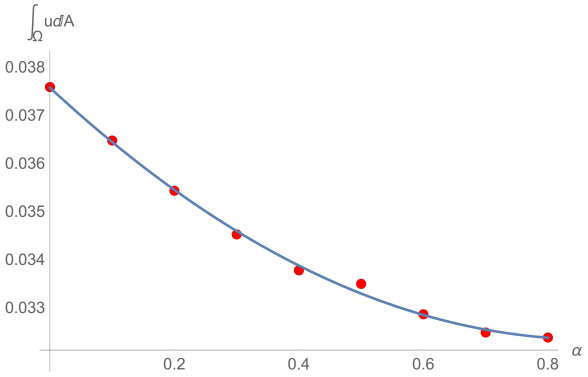

FIGURE 5: Total biofilm concentration $u_{vol}(T;\alpha) := \int_\Omega u\,dA$ Vs α for final time: $T = 0.6$. Dots: computed values. Solid line: Best-fit curve using MATLAB's 'cftool' package: $u_{vol}(T;\alpha) = 0.006878\alpha^2 - 0.012\alpha + 0.03757$ (Goodness of fit: SSE: 6.018e-08, R-square: 0.9978). Governing parameters: $D_n = 0.1$, $D_b = 0.001$, $K = 0.5$, $r_b = r_n = 10$. Initial conditions: $u_0 = 0.1$ on $D = \{(x,y) \in \mathbb{R}^2 \mid (x-0.5)^2 + (y-0.8)^2 = 0.01\}$ and $u_0 = 0$ elsewhere

CONCLUSION AND ONGOING DIRECTIONS

We developed a model for bacterial colony growth incorporating the effect of the gravitational field. We investigated the case of a single spherical colony consisting of non-motile bacteria suspended in an aqueous solution. The

associated governing system of nonlinear PDEs was solved numerically using the DG-FE method for the spatial discretization and the theta method for the time discretization. We found that the colony progressively grew at a faster rate as the intensity of the gravitational field was reduced to zero. Published experimental data comparing microgravity and normal gravity - that are readily available - were found to be in qualitative agreement with our results. In addition, a quantitative relationship between the biofilm volume fraction and the gravitational constant was derived. It was also observed that the colony acted as a nutrient sink. Furthermore, nutrient concentration was reduced in the region directly below. This phenomenon was significantly more pronounced for non-zero gravity. As a topic of future work, we are investigating the case of multiple colonies and their interactions, including the final stage of sedimentation where colonies reach the bottom of the tank.

ACKNOWLEDGEMENTS

The work of N. C. Papanicolaou was partially supported by the Scientific Foundation of the Republic of Bulgaria under grant DFNI I-02/9. A. C. Aristotelous gratefully acknowledges partial financial support from the National Science Foundation under Grant DMS-1720226.

REFERENCES

[1] D. W. Koenig and D. L. Pierson (1997) *Water Sci. Technol.* **35**.
[2] D. Pierson, R. Bruce, C. M. Ott, V. Castro, and S. Mehta, "Microbiological lessons learned from the space shuttle," in *41st International Conference on Environmental Systems, (ICES)*, AIAA Meeting Papers (American Institute of Aeronautics and Astronautics, Reston, VA, 2011), pp. *AIAA* (2011) **5266**, 1–11.
[3] N. D. Novikova (2004) *Microb. Ecol.* **47**, 127–132.
[4] B. Song and L. G. Leff (2005) *Microbiol. Res.* **160**, 111–117.
[5] J.-D. Gu (2003) *Int. Biodeter. Biodegr.* **52**, 69–91.
[6] A. Matin and S. Lynch (2005) *ASM News* **71**, 235–240.
[7] N. Novikova, P. D. Boever, S. Poddubko, E. Deshevaya, N. Polikarpov, N. Rakova, I. Coninx, and M. Mergeay (2006) *Res. in Microbiol.* **157**, 5–12.
[8] C. M. Oubre, D. L. Pierson, and C. M. Ott, "Microbiology," in *Space Physiology and Medicine: From Evidence to Practice*, edited by A. E. Nicogossian *et al* (Springer, New York, 2016), pp. 155–167.
[9] J.-D. Gu (2007) *Int. Biodeter. Biodegr.* **59**, 170–179.
[10] A. Matin, S. Lynch, and M. Benoit (2006) *Gravit. Space Biol.* **19**, 31–42.
[11] S. V. Lynch, K. Mukundakrishnan, M. R. Benoit, P. S. Ayyaswamy, and A. Matin (2006) *Appl. and Environ. Microbiol.* **72**, 7701–7710.
[12] L. Mauclaire and M. Egli (2010) *FEMS Immunol. Med. Microbiol.* **59**, 350–356.
[13] F. Mastroleo, R. V. Houdt, S. Atkinson, M. Mergeay, L. Hendrickx, R. Wattiez, and N. Leys (2013) *Microbiology* **159**, 2456–2466.
[14] M. E. Hummerick, J. L. Coutts, G. M. Lunn, L. S. Spencer, C. L. Khodadad, and S. Frances, "Dormancy and recovery testing for biological wastewater processors," in *45th International Conference on Environmental Systems, (ICES)*, AIAA Meeting Papers (American Institute of Aeronautics and Astronautics, Reston, VA, 2015), pp. ICES (2015) **197** 1–11.
[15] D. M. Klaus (2001) *Gravit. Space Biol. Bull.* **14**, 55–64.
[16] T. G. Hammond and J. M. Hammond (2001) *Am. J. Physiol. Renal. Physiol.* **281**, F12–F15.
[17] C. A. Nickerson, C. M. Ott, J. W. Wilson, R. Ramamurthy, and D. L. Pierson (2004) *Microbiol. Mol. Biol. Rev.* **68**, 345–361.
[18] E. E. Higginson, J. E. Galen, M. M. Levine, and S. M. Tennant (2016) *Pathog. Dis.* **74**, ftw095: 1–9.
[19] M. Lappa, "Ch. 7: The growth of biological tissues," in *Fluids, Materials and Microgravity: Numerical Techniques and Insights into Physics*, (Elsevier Science, 2005), pp. 453–484.
[20] D. A. Wolf and S. J. Kleis, "Ch. 2: Principles of analogue and true microgravity bioreactors to tissue engineering," in *Effect of Spaceflight and Spaceflight Analogue Culture on Human and Microbial Cells*, (Springer, New York, 2016), pp. 453–484.
[21] H. Gao, P. Ayyaswamy, and P. Ducheyne (1997) *Microgravity Sci. Technol.* **10**, 154–165.
[22] E. A. Nauman, C. M. Ott, E. Sander, D. L. Tucker, D. Pierson, J. W. Wilson, and C. A. Nickerson (2007) *Appl. Environ. Microbiol.* **73**, 699–705.

[23] C. M. Begley and S. J. Kleis (2000) *Biotechnol. Bioeng.* **70**, 32–40.
[24] M. Lappa (2003) *Biotechnol. Bioeng.* **84**, 518–532.
[25] T.-C. Chao and D. B. Das (2015) *Chem. Eng. J.* **259**, 961–971.
[26] M. A. Kacena, G. A. Merrell, B. Manfredi, E. E. Smith, D. M. Klaus, and P. Todd (1999) *Appl. Microbiol. Biotechnol.* **51**, 229–234.
[27] D. Klaus, S. Simske, P. Todd, and L. Stodieck (1997) *Microbiology* **143**, 449–455.
[28] E. S. Nelson, NASA Technical Memorandum 103775, 1991.
[29] NASA, Microgravity science on the ISS: A primer for new researchers, `https://www.nasa.gov/pdf/501343main_Microgravity_Science.pdf`, 2015, Online, NASA Website; accessed 2-May-2015.
[30] I. Klapper and J. Dockery (2010) *SIAM Rev.* **52**, 221–265.
[31] G. K. Batchelor, *An Introduction to Fluid Dynamics* (Cambridge University Press, Cambridge, U.K., 2001), pp. 230–235.
[32] A. Haider and O. Levenspiel (1989) *Powder Technol.* **58**, 63–70.
[33] A. C. Aristotelous, I. Klapper, Y. Grabovsky, B. Pabst, B. Pitts, and P. S. Stewart (2015) *Phys. Rev. E***92**, paper 022703, 7p.
[34] A. C. Aristotelous and M. Haider (2014) *Int. J. Numer. Meth. Biomed. Eng.* **30**, 767–780.
[35] D. N. Arnold, F. Brezzi, B. Cockburn, and L. D. Marini (2002) *SIAM J. Numer. Anal.* **39**, 1749–1779.
[36] B. Riviére, *Discontinuous Galerkin Methods for Solving Elliptic and Parabolic Equations* (SIAM, Philadelphia, 2008).
[37] W. Bangerth, T. Heister, L. Heltai, G. Kanschat, M. Kronbichler, M. Maier, B. Turcksin, and T. D. Young (2015) *Archive of Numerical Software* **3**.
[38] W. Bangerth, R. Hartmann, and G. Kanschat (2007) *ACM Trans. Math. Softw.* **33**, 24/1–24/27.
[39] I. Klapper and J. Dockery (2006) *Phys. Rev. E***74**, 031902, 8p.